

sMark

lato<sup>1</sup>,  
anzano Garcia<sup>1</sup>,  
Sarah Elderkin<sup>1</sup>,

**B**



were correlated between pro- and pre-B cells, even when significance was reached in only one of the cell types (Fig. 2c). Several of the age-upregulated genes, particu-

genes from further analyses and chose to focus primarily on age-downregulated genes, since we are confident that they do not arise from this potential contamination.

Many genes with age-associated changes in expression also showed a strong modulation of their expression during B cell development (Additional file 2: Figure S1a). Genes whose expression decreased upon aging in pro-B cells were frequently downregulated during the pro-B to pre-B cell transition in young cells (Additional file 2: Figure S1a, blue points); examples include *2*,

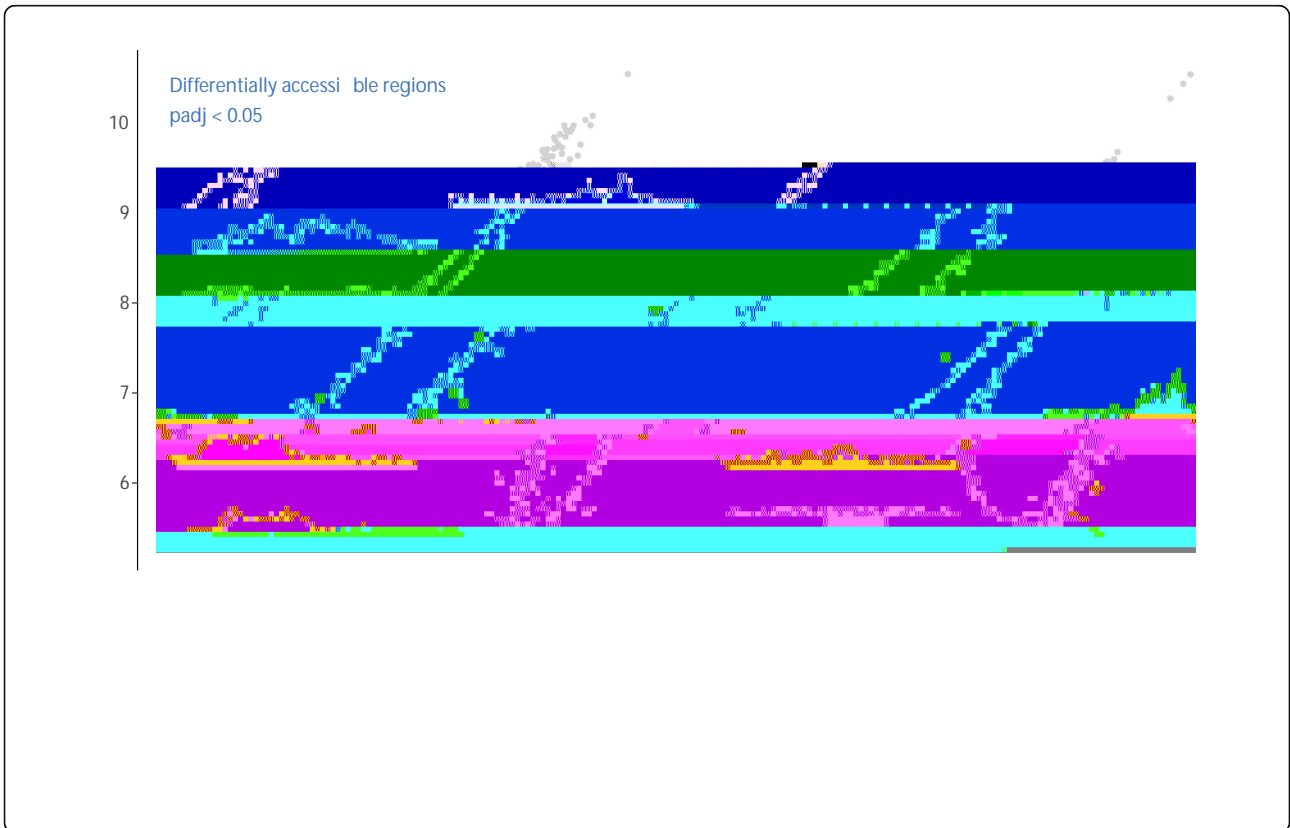
Additional file 2: Figure S1a, 42

Additional file 2: Figure S1b). This pattern suggests a failure to upregulate these genes as the aged B cell progenitors progress to the pre-B cell stage. Notably, several genes downregulated upon aging at the pro-B and/or pre-B cell stage encode components of the IGF signaling pathway, such as *IRS1* and *IGF1R*. Indeed, *IRS1*, a key component of this pathway, was found to be the most significantly downregulated gene in pre-B cells upon aging at the messenger RNA (mRNA) level. We therefore examined *IRS1* protein levels and found that these were decreased upon aging in both pro-B and pre-B cells (Fig. 2d), demonstrating that age-specific mRNA changes of *IRS1* are propagated into reduced protein levels.

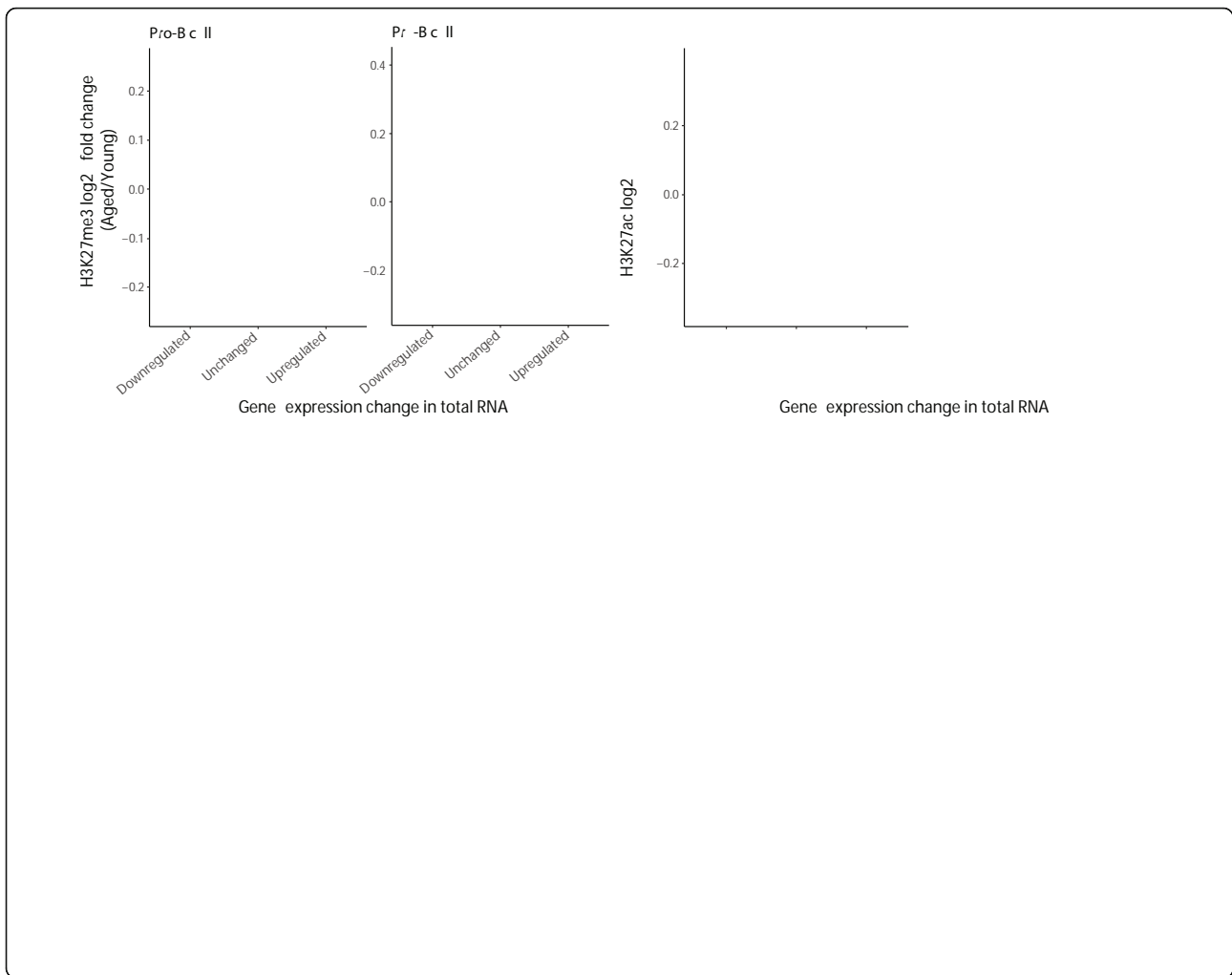
Total RNA levels reflect both the rate of transcription and downstream processes such as RNA stability. To explore the effects of aging on gene transcription more directly, we isolated nuclear RNA from young and aged pro-B cells to enrich for nascent transcripts and profiled global changes in intronic transcription as a specific measure of nascent transcription. While ~17% (30 out of 175) of DEGs detected in total RNA were also DEGs in the nuclear RNA-sequencing (RNA-seq) analysis, and overall the fold changes were correlated (Additional file 2: Figure S2), this analysis revealed many more genes showing significant age-related differential transcription (Fig. 3a; Additional file 1: Table S4; 147 downregulated and 255 upregulated genes upon aging). Notably, several age-

downregulated genes, such as *IRS2* [18], *IGF1R*, *IGF2*, *IGF3*, and *IGF1*, and upregulated genes, such as *IGF1R* [19] and *IGF1R3* [20], have been linked to IGF signaling or type 2 diabetes. More broadly, KEGG pathway analysis of DEGs highlighted several metabolic pathways linked to nutrient signaling (Additional file 2: Figure S3).

The nuclear RNA-seq analysis revealed *miR-29b-2* as one of the most significantly downregulated genes in aged pro-B cells (Fig. 3a, Additional file 2: Figure S4a). *miR-29b-2* is a non-coding transcript implicated in the regulation of imprinting and serves as the non-coding precursor RNA of miRNAs *miR-29b-1* and *miR-29b-2* [21, 22]. To explore the link between miRNA expression and aging in B cell precursors, we performed small RNA-seq. We identified 34 significantly differentially expressed miRNAs in either pro- or pre-B cells (Fig. 3b, c; Additional file 1: Table S5). Of these, 20.6% (7 out of 34) were differentially expressed in both pro- and pre-B cells. This analysis confirmed a profound downregulation of *miR-29b-1* and *miR-29b-2*, consistent with changes in *miR-29b-2* levels detected with nascent RNA-seq. We also observed an upregulation of seven *miR-145*-family members and of *miR-123*, upon aging in pro- and/or pre-B cells (Fig. 3b, c). Differentially expressed miRNAs segregated into clusters displaying similar expression changes upon aging, several of which also showed a modulation in their expression between pro-B and pre-B cells (Fig. 3c).



KEGG pathway analysis of validated target genes of the differentially regulated miRNAs (Additional file [1](#))



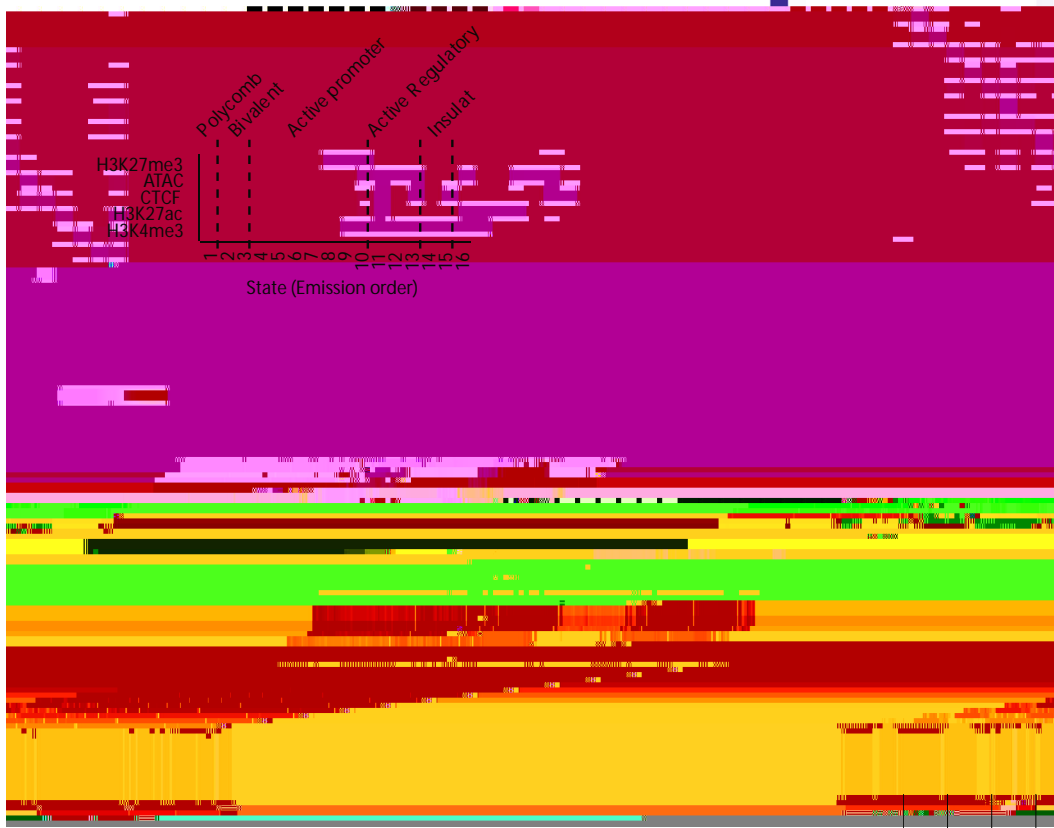
cells appears to arise due to a failure to relieve polycomb-mediated silencing in the transition from the pro-B to the pre-B cell stage.

Acetylation at lysine 27 of histone H3 is mutually exclusive to methylation of this residue and is linked to active enhancers or promoters. We noted a trend towards increased H3K27ac enrichment at peaks overlapping or within 10-kb of the upregulated genes in the aged pro-B and pre-B cells, while the opposite was true for downregulated genes (Additional file 2: Figure S6d). Notably, H3K27ac displayed reciprocal changes to H3K27me3 at the promoter of *1* and the *1-2* precursor (Additional file 2: Figures S6d, S8, and S9). Analysis of CTCF ChIP-seq data did not reveal any significant differential binding of CTCF between young versus aged pre-B cells (Additional file 2: Figure S6e).

The stringent threshold-based approach presented above identified high-confidence loci showing changes in chromatin accessibility and histone modifications upon aging, revealing remarkably few such changes, but highlighting a significant chromatin component to the

transcriptional regulation of *1* and the *1-2* miRNAs. However, this does not exclude the possibility that more subtle changes in the epigenomic landscape might play a broader role in shaping the gene expression profile of aged compared to young B cell precursors. Therefore, we tested whether changes in chromatin, identified using a low stringency threshold, were generally accompanied by altered gene expression (Additional file 2: Figure S10; Additional file 1: Tables S6–S9) and whether genes with altered expression were characterized by remodelled chromatin (Fig. 5). This revealed not only that changes in chromatin upon aging, especially H3K4me3 and H3K27me3 occupancy, likely impact on gene expression (Additional file 2: Figure S10), but further, that if there is a change in gene expression, this is frequently linked to changes in chromatin (Fig. 5). It is noteworthy that H3K4me3 and H3K27ac agree more with differential gene expression than chromatin accessibility (ATAC-seq; Fig. 5; Additional file 2: Figure S10). This is in line with the fact that chromatin accessibility is not necessarily linked to active gene expression but can also be found

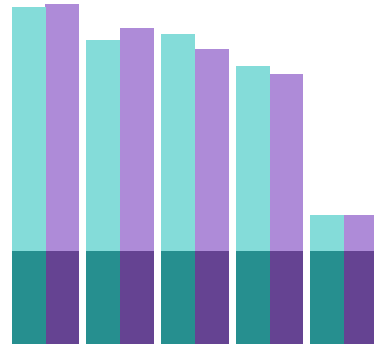
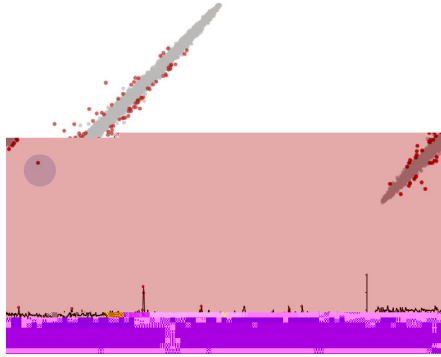




|  |  |  |  |  |
|--|--|--|--|--|
|  |  |  |  |  |
|  |  |  |  |  |
|  |  |  |  |  |
|  |  |  |  |  |




a



transitioned to a bivalent state upon aging (Fig. 6d); it was also identified in the genome-wide analysis, segregating in cluster 2 (Fig. 6c). Chromatin state analysis thus highlights genes that show the most profound alterations in the chromatin at their promoters.

Taken together, these results demonstrate specific age-associated changes in the chromatin at gene promoters in developing B cells, which potentially underlie the observed age-specific changes in gene expression.



Aging has been linked with changes in genome organization in other systems [29]. In order to address whether such changes occur in developing B cells and whether these correlate with changes in gene regulation, we first performed Hi-C in nuclei isolated from pre-B cells. We used Hi-C data to segment the genomes into A (active) and B (repressed) compartments using principal component analysis (PCA) combined with H3K4me3 data [30]. This analysis showed that the chromosome compartmentalization was near identical between young and aged pre-B cells. However, 100 out of 9928 regions displayed a significant change in their compartment score upon aging (Fig. 7a top left; Additional file 1

examples of such ‘rewiring’ of interactions included the age-downregulated *U1* gene, which lost several interactions in aged cells, including an interaction with the highly active chromatin surrounding the *U3* promoter (Fig. 8a; Additional file 2: Figure S13b).

These results suggest that modulation of the chromatin at PIRs occurs infrequently in aging, even when the expression from the promoter is altered. Rather, our analysis reveals that gene expression changes upon aging are frequently linked to ‘rewiring

interactions, that might contribute to the broader shifts

additional pathways that may be revealed by analysis of individual mice, we believe we have captured dominant pathways that are altered in aging mouse B cell precursors.

Our analyses revealed alterations in the IGF signaling pathway at several regulatory levels, suggesting a pivotal contribution to the aging process in B cell precursors. We observed changes in the expression of several key components of the insulin/IGF signaling (IIS) machinery, especially *Ins1* and *Ins2*, with striking alterations in the chromatin and interaction profile at the *Ins1* promoter/regulatory regions, underscoring that this regulation is in part at the transcriptional level and involves polycomb-mediated repression. We also observed decreased IRS1 protein levels in the aged pro- and pre-B cells compared with the young cells, demonstrating that the lower mRNA level leads to a reduction in the amount of IRS1 protein produced. Notably, downregulation of these key players in the IIS and nutrient signaling pathways has been associated with the aging process, as further discussed below.

Several of the differentially expressed miRNAs that we identified have also been linked to insulin/IGF/metabolic signaling. These include miR-223, which modulates *Ins1* expression [39, 40], and the miR-101 miRNA family, which regulates *Ins1*. miR-101 miRNAs are critical regulators of glucose metabolism and insulin signaling; the upregulation of miR-101 expression leads to downregulation of expression of several components of the insulin signaling machinery in skeletal muscle and liver, such as *Ins1* and *Ins2* [41, 42]. We predict that the increased abundance of miR-101 in aged B cell precursors would drive a decrease in IIS responsiveness, through targeting *Ins1* and other components at the post-transcriptional level. Notably, we also observed striking alterations in the chromatin at a novel potential precursor RNA for the miR-101 and miR-102 miRNAs, indicative of an interplay between epigenetic and post-transcriptional mechanisms in shaping gene expression.


The gene expression changes we observed in developing 9he0Insighlif(ctio331(mt(r)749(toe)-350statu999976729999(below.))niche,299(to)-12.6.89999(th)-420.othenti30down)-8.facto/)TJ,se

particular, we found unaltered expression of the IL7R, consistent with previous studies implicating reduced availability of IL7 and cytoplasmic signaling of the IL7R in the reduction of pro-B cell numbers in aging [13, 57]. Additionally, we did not detect altered expression of SL components of the pre-BCR. Reduced SL cell surface expression observed in aged precursor B cells has been proposed to be an adaptive response to the aging micro-environment which restricts pre-B cell selection [58]. Our data suggest that neither of these pathways is dys-regulated at the level of gene expression in aging B cell precursors.

It is noteworthy that  $I^{-/-}$  mice have a longer life- and health-span, with an aged T cell profile that is more comparable to young mice than the control aged mice [44, 45]



default parameters [64]. To identify populations of interest, manual gates were projected onto the tSNE plot.

  
For nuclear RNA-seq, nuclei were isolated from 1 to  $10 \times 10^6$  flow sorted B lymphocytes by incubation in 50 mM Tris-HCl pH 7.5, 140 mM NaCl, 1.5 mM  $MgCl_2$ , 1 mM DTT, 0.4% NP40 for 5 min on ice followed by centrifugation at  $500 \times g$ . RNA was isolated with a RNeasy mini kit (Qiagen) and treated with Turbo DNase (Ambion). Total RNA was isolated and depleted of rRNA using a Ribo-Zero Gold rRNA removal kit (Human/Mouse/Rat; Illumina) according to the manufacturer's instructions.

9.4(9e559.0504995-14/ottr)-9.h4995-9.40002(nuc2(ar)6980.79998(and57099(total57005.29999(RNA)--8.,(d)]TJ1.2

Amplification kit (KAPA, Cat. KK2501) using 15 cycles. Libraries were sequenced on a HiSeq2500 sequencer (Illumina) according to manufacturer's instructions.

- e - ( - )  
Hi-C and PHi-C libraries were generated as described [32] with modifications as detailed below. In total,  $3.2$  to  $3.5 \times 10^7$  pre-B cells were fixed in 2% formaldehyde (Agar Scientific) for 10 min, after which the reaction was

PE PCR 2.0 primers (Illumina). After PCR amplification, the Hi-C libraries were purified with AMPure XP beads (Beckman Coulter). The concentration of the Hi-C libraries was determined by Bioanalyzer profiles (Agilent Technologies) and qPCR (Kapa Biosystems); the Hi-C libraries were paired-end sequenced (HiSeq 1000, Illumina) at the Babraham Institute Sequencing Facility.

For PCHi-C, 500 ng of Hi-C library DNA was resuspended in 3.6 L H<sub>2</sub>

have been considered. The identified target genes for each class have been used for KEGG pathway analysis using DAVID v6.8 online server [75, 76].  $p$  values reflect multiple-test corrected (Benjamini–Hochberg) values.

4

Trimmed reads were aligned to the GRCm38 mouse reference genome using Bowtie 2 [73]. Reads mapping to the mitochondrial genome and alternative contigs were excluded from downstream analysis. Fragment size analysis and quality control was made by a custom in-house code. Fragment coverage BigWig files were constructed using bedtools V2 [77].

We used MACS2 [78, 79] with ‘--nomodel --shif -25 --extsize 50 -q 0.01’ for detection of open chromatin (peaks of read counts). With these parameters, we detected 18,000–51,000 peaks per sample. For each condition (young and aged), a region was accepted as a condition-specific peak if the region was detected as a peak in at least three out of four samples. Two peaks closer than 100-bp to each other were merged. We further pooled young and aged peak sets to get a genome-wide set (union) of open chromatin regions for further differential accessibility analysis. After removing reads with a mapping quality score  $< 30$ , peaks were filtered to exclude those with  $< 64$  reads or that overlapped with a blacklisted region [80, 81]. We used featureCounts [82] to count the number of fragments overlapping these regions in each sample. We used DESeq2 [70] for detection of differentially accessible regions, with an adjusted

of chromatin states in the range of 3–24. We chose 16 states as the optimum; these were then manually collapsed into six distinct and more biologically relevant

mapped to the baited [genomic](#) fragment encompassing the *I* gene promoter. Read counts were quantified over merged [genomic](#) fragments, such that each quantitation window comprised five adjacent [genomic](#) fragments.

Pre- and pro-B cell pellets were sonicated in SDS sample buffer and proteins resolved by SDS-PAGE. Proteins were transferred onto PVDF membranes and immunoblotted with the indicated primary antibodies at 4 °C overnight, followed by 1 h at room temperature. Membranes were washed in TBST (40 mM Tris-HCl, pH 8.0 at room temperature; 0.14 M NaCl; 0.1% Tween-20) and incubated with HRP-conjugated secondary antibodies. IRS1 antibody #2382 was from Cell Signaling Technology (CST)/New England Biolabs (NEB); anti-beta-COP antibody was a kind gift from Dr. Nick Ktistakis, Babraham Institute, UK; goat Anti-Rabbit and anti-Mouse IgG (H + L)-HRP conjugate was from BioRad. Membranes were washed and signal detected by enhanced chemiluminescence. Relative protein expression was quantified using Aida 2D Densitometry software (v3.27).

## A

- [A](#) [1](#) [1](#) [1](#) **1:** Supplementary Tables S1–S16. XLSX file describing datasets generated for this study. (XLSX 369 kb)
- [A](#) [1](#) [1](#) [2](#) **2:** Supplementary Figures S1–S15. PDF of all supplementary figures S1–S15. (PDF 4237 kb)
- [A](#) [1](#) [1](#) [3](#) **3:** Chromatin segmentation output for young pre-B cells. TXT file listing chromatin segmentation output for young pre-B cells. (TXT 4627 kb)
- [A](#) [1](#) [1](#) [4](#) **4:** Chromatin segmentation output for aged pre-B cells. TXT file listing chromatin segmentation output for aged pre-B cells. (TXT 4190 kb)
- [A](#) [1](#) [1](#) [5](#) **5:** Reviewer reports and authors' response to reviewers. (DOCX 119 kb)

DEG: Differentially expressed gene; IGF: Insulin-like growth factor; IIS pathway: Insulin/insulin-like growth factor signaling pathway; IL7R: Interleukin 7 receptor; miRNA: MicroRNA; PCHI-C: Promoter Capture Hi-C; PIR: Promoter interacting region; pre-BCR: Pre-B cell receptor; SD: Standard deviation; SL: Surrogate light chain; tSNE: t-Distributed Stochastic Neighbor Embedding

We thank Olga Mielczarek, Amanda Baizan-Edge, Bryony A. Stubbs, and Keith M. Porter for their help in collecting cells and Kristina Tabbada, Babraham

6. Bednarski JJ, Pandey R, Schulte E, White LS, Chen B-R, Sandoval GJ, et al. RAG-mediated DNA double-strand breaks activate a cell type-specific checkpoint to inhibit pre-B cell receptor signals. *J Exp Med.* 2016;213:209–23.
  7. Landreth KS, Narayanan R, Dorshkind K. Insulin-like growth factor-I regulates pro-B cell differentiation. *Blood.* 1992;80:1207–12.
  8. Cancro MP, Hao Y, Scholz JL, Riley RL, Frasca D, Dunn-Walters DK, et al. B cells and aging: molecules and mechanisms. *Trends Immunol.* 2009;30:313–8.
  9. Stephan RP, Sanders VM, Witte PL. Stage-specific alterations in murine B lymphopoiesis with age. *Int Immunol.* 1996;8:509–18.
  10. Labrie JE, Sah AP, Allman DM, Cancro MP, Gerstein RM. Bone marrow microenvironmental changes underlie reduced RAG-mediated recombination and B cell generation in aged mice. *J Exp Med.* 2004;200:411–23.
  11. Kline GH, Hayden TA, Klinman NR. B cell maintenance in aged mice reflects both increased B cell longevity and decreased B cell generation. *J Immunol.* 1999;162:3342–9.
  12. Johnson KM, Owen K, Witte PL. Aging and developmental transitions in the B cell lineage. *Int Immunol.* 2002;14:1313–23.
  13. Stephan RP, Lill-Elghanian DA, Witte PL. Development of B cells in aged mice: decline in the ability of pro-B cells to respond to IL-7 but not to other growth factors. *J Immunol.* 1997;158:1598–609.
  14. Moskowitz DM, Zhang DW, Hu B, Le Saux S, Yanes RE, Ye Z, et al. Epigenomics of human CD8 T cell differentiation and aging. *Sci Immunol.* 2017;2:eaag0192.
  15. Ucar D, Márquez EJ, Chung C-H, Marches R, Rossi RJ, Uyar A, et al. The chromatin accessibility signature of human immune aging stems from CD8 +T cells. *J Exp Med.* 2017;214:3123–44.
  16. Miller JP, Allman D. The decline in B lymphopoiesis in aged mice reflects loss of very early B-lineage precursors. *J Immunol.* 2003;171:2326–30.
  17. Agoulnik IU, Hodgson MC, Bowden WA, Ittmann MM. INPP4B: the new kid on the PI3K block. *Oncotarget.* 2011;2:321–8.
  18. Jin T, Li J, Wei J, Xu P, Yan M, Li J, et al. Impact of diabetes-related gene polymorphisms on the clinical characteristics of type 2 diabetes Chinese Han population. *Oncotarget.* 2016;7:85464–71.
- 199999190.5 Exp reflects

57. Sherwood EM, Xu W, Riley RL. B cell precursors in senescent mice exhibit decreased recruitment into proliferative compartments and altered expression of Bcl-2 family members. *Mech Ageing Dev.* 2003;124:147–53.
58. Ratliff M, Alter S, McAvoy K, Frasca D, Wright JA, Zinkel SS, et al. In aged mice, low surrogate light chain promotes pro-B-cell apoptotic resistance, compromises the PreBCR checkpoint, and favors generation of autoreactive, phosphorylcholine-specific B cells. *Aging Cell.* 2015;14:382–90.
59. Cohen E, Paulsson JF, Blinder P, Burstyn-Cohen T, Du D, Estepa G, et al. Reduced IGF-1 signaling delays age-associated proteotoxicity in mice. *Cell.* 2009;139:1157–69.
60. Kramer NJ, Wang W-L, Reyes EY, Kumar B, Chen C-C, Ramakrishna C, et al. Altered lymphopoiesis and immunodeficiency in miR-142 null mice. *Blood.* 2015;125:3720–30.
61. Knoll M, Simmons S, Bouquet C, Grün JR, Melchers F. miR-221 redirects precursor B cells to the BM and regulates their residence. *Eur J Immunol.* 2013;43:2497–506.
62. Costinean S, Zanesi N, Pekarsky Y, Tili E, Volinia S, Heerema N, et al. Pre-B cell proliferation and lymphoblastic leukemia/high-grade lymphoma in E(mu)-miR155 transgenic mice. *Proc Natl Acad Sci*